Journal of Fluorine Chemistry 144 (2012) 124–129

Contents lists available at SciVerse ScienceDirect

Journal of Fluorine Chemistry

journal homepage: www.elsevier.com/locate/fluor

Effect of fluorine–oxygen mixed gas treated graphite fibers on electrochemical behaviors of platinum–ruthenium nanoparticles toward methanol oxidation

Soo-Jin Park [a], Yongju Jung [b], Seok Kim [c,*]

[a] Department of Chemistry, Inha University, 253, Yonghyun-dong, Nam-gu, Incheon 402-751, South Korea
[b] Department of Applied Chemical Engineering, Korea University of Technology and Education, 307, Gajeon-ri, Byeongcheon, Cheonan-si, Chungnam-do 330-708, South Korea
[c] School of Chemical and Biomolecular Engineering, Pusan National University, San 30, Jangjeon-dong, Gemjeong-gu, Busan 609-735, South Korea

ARTICLE INFO

Article history:
Received 16 March 2012
Received in revised form 21 August 2012
Accepted 22 August 2012
Available online 30 August 2012

Keywords:
Gas treatment
Graphite fibers
Platinum–ruthenium
Catalysts
Electroactivity

ABSTRACT

In the present study, graphite fibers (GFs) were treated with fluorine–oxygen mixed gas with changing gas treatment temperatures to study the effect of surface modification. Treated GFs-supported platinum (Pt)/ruthenium (Ru) catalysts were prepared to check the influence of gas treatment on electroactivity of metal catalysts. The crystalline size and the surface compositions of the carbon-supported catalysts were determined by XRD and XPS, respectively. Electrochemical properties of the electrocatalysts were analyzed by cyclic voltammetry (CV) measurements. When gas-treated GFs were used as a catalyst support, the current density for a methanol oxidation was greater than that of pristine catalyst; meaning the treated GFs-supported catalysts had a higher electroactivity. These results were in agreement with CV results that confirmed the greater effective electrochemical surface area for a hydrogen adsorption–desorption reaction of catalysts, which was originated from smaller particle size.

1. Introduction

During the last decade there have been extensive efforts in the research of the catalysts for an electrochemical oxidation of methanol and the development of the direct methanol fuel cells (DMFCs) [1–5]. Direct injection of the methanol fuel would avoid the problems that are related to the production, purification and storage of hydrogen. However, the performances of DMFCs are still limited by several problems, including the poor kinetics of both the anodic and the cathodic reactions. Pt has been shown to be the only active and stable single metal catalyst for dissociative chemisorptions of methanol in acidic media, but it is very sensitive to CO poisoning, which are formed by the initial dehydrogenation of the methanol molecules. On the other hand, the enhanced activity of Pt–Ru compared to Pt for methanol oxidation has been attributed to both electronic and bifunctional effects [6–10]. In DMFCs systems, interest has also been focused on the development of a supporting material, one of the key factors in increasing the utilization of noble metal catalysts. The particle shape, size and size-distribution are important in influencing an electrocatalytic activity of carbon-supported Pt or Pt-based alloys [11,12].

In fact, the choice of a suitable supporting material is a critical factor that may affect the performance of supported electrocatalysts owing to interactions and surface reactivity. Carbon materials are widely used as support materials. Whereas carbon blacks are the common support materials for electrocatalysts, new forms of carbon materials such as carbon fibers or graphite fibers (GFs) and carbon nanotubes (CNTs) have been investigated as catalyst supports [13–19]. In recent years, fluorine or oxygen treatment has been investigated as an interesting surface modification tool. In comparison with other surface modification techniques, fluorine or oxygen atoms penetrate the material surfaces to relatively large depths that are controllable [20–25]. These kinds of surface-modified support effect on the preparation and electroactivity of deposited catalysts were not fully analyzed and systematically characterized.

In the present study, the surface modifications of graphite fiber supports were studied to monitor the treatment effect on the size and the loading efficiency of post-deposited platinum–ruthenium particles, determining the electroactivity of catalysts. Graphite fiber-supported platinum (Pt)–ruthenium (Ru) catalysts nanoparticles were prepared by changing the temperature of fluorine or oxygen gas treatment to check the influence of gas treatment intensity on the electroactivity of catalysts.

2. Experimental

2.1. Materials and surface modification of carbon materials

The graphite fibers (GFs) were used as a support for the metal catalysts. GFs which were supplied by Showa Denko Co. (Japan). These carbon fiber materials have a diameter of 100–150 nm and a

* Corresponding author. Tel.: +82 51 510 3874; fax: +82 51 512 8563.
E-mail address: seokkim@pusan.ac.kr (S. Kim).

0022-1139/$ – see front matter © 2012 Elsevier B.V. All rights reserved.
http://dx.doi.org/10.1016/j.jfluchem.2012.08.003

length of 5–50 μm, resulting in a large aspect ratio. The product code is VGCF-H. The graphite fibers have a density of 0.08 g/cm^3 and specific surface area of 13 m^2/g. It has a resistivity of 10^{-4} Ohm cm. Chloroplatinic acid (H_2PtCl_4) and ruthenium chloride ($Ru(OH)_3$) catalysts were purchased from Aldrich. The reducing agent, HCHO (35%), was also obtained from Aldrich. Before catalyst deposition, GFs were subjected to treatment at different temperatures (RT ~ 300 °C) under fluorine and oxygen mixed gas (mole ratio = 80:20) flow in order to realize their different Pt and Ru loading contents, respectively. The mixed gas pressure was fixed to 0.1 MPa, and the nominal reaction time was fixed to 15 min at the given treatment temperature. We have assigned carbon sample names such as pristine GFs, GFs-RT, GFs-100, GFs-200, GFs-300.

2.2. Catalyst preparation

The carbon materials-supported Pt and Ru catalysts were prepared by chemical reduction of Pt/Ru colloids in an aqueous solution using HCHO as a reducing agent. Prior to using the as-received GFs, the metal catalysts used in the synthesis and the amorphous carbons were removed by two-step purification: exposure at 500 °C in an O_2 stream for 90 min and soaking in 5 M HNO_3 for 3 h. These purified GFs were named as pristine GFs.

Gas-treated carbon materials (125 mg) were suspended in 25 ml of deionized water and stirred. Separately, 58.3 mg of H_2PtCl_4 and 30 mg of $Ru(OH)_3$ in dissolved deionized water was slowly added dropwise to the above solution which was stirred mechanically for 1 h. A 5 M NaOH aqueous solution was added to adjust the pH of the mixture to 12–13 approximately. Then, HCHO (37%, 0.75 ml) was added to the solution to reduce the Pt and Ru, Reduction reaction was performed by heating the mixture solution at 80 °C for 1 h, during which high purity argon gas was passed through the reaction system to remove the organic by-products. After cooling to the room temperature, the resultant catalyst was washed with distilled water and ethanol. The obtained powder was dried in a vacuum oven at 70 °C for 24 h.

2.3. Physical and chemical characterization

X-ray photoelectron spectroscopy (XPS) of samples was analyzed using a VG Scientific LAB MK-II spectrometer. The pressure in the sample chamber was controlled in the range 10^{-8}–10^{-9} Torr. The binding energies was detected in the range of 0–1100 eV.

The carbon and fluorine loading level was calculated by the energy dispersive X-ray spectroscopy (EDS) method, considering the atomic ratio of the carbon and fluorine intensity. X-ray diffraction (XRD) analysis with a Rigaku D/MAX-2200V diffractometer using a Cu Kα (λ = 0.15406 nm) source operating at 40 kV and 40 mA, was carried out on catalysts from different precursors. The XRD patterns were plotted at a scanning rate of 4°/min with an angular resolution of 0.05° for the angle scan. The X-ray diffractograms were obtained for 2θ values varying between 10° and 100°.

The loading masses of the Pt and Ru were determined using an inductively coupled plasma-atomic emission spectrometer (ICP-AES) using a Jobin Yvon Ultima C-spectrometer. Carbon-supported particles were diluted 1:20 with 2% HNO_3 in triplicate.

For the direct determinations of the major elements in samples, each sample was diluted (v/v, 1:20) with 2% HNO_3 in triplicate. Furthermore, dilutions of 1:5 and 1:10 were tested for their applicability. The resulting clear solutions were then brought to 20 ml with double distilled water.

Transmission electron microscopy (TEM) photographs of the catalyst samples were taken by 1-nm spatial-resolution TEM. Before taking the electron micrographs, the catalyst samples were ultrasonically dispersed in isopropyl alcohol, and a drop of the resultant dispersion was deposited and dried on a standard copper-grid coated with a polymer film. The applied voltage was 100 kV for the catalysts.

2.4. Electrochemical characterization

Electrochemical measurements were carried out on a conventional three electrode electrochemical cell at 25 °C. A conventional three-compartment electrochemical cell was employed for all electrochemical tests. A KCl-saturated Ag/AgCl electrode was used as the reference electrode and a platinum wire as the counter electrode. All electrochemical tests were carried out at room temperature. Glassy carbon (GC) electrode (Bioanalytic Systems, Inc., 3-mm diameter) was used as a substrate for the working electrode. We prepared a working electrode by coating the catalyst powder mixed with Nafion® polymer (5 wt.%, Aldrich) onto a glassy carbon electrode. The solution of 1 M CH_3OH and 0.5 M H_2SO_4 was stirred constantly and purged with ultra-pure argon gas. Electrochemical experiments were performed using Autolab with PGSTAT 30 (Eco Chemie, The Netherlands), an electrochemical analysis instrument. A cyclic potential was swept between −0.2 V and 0.8 V vs. Ag/AgCl with a scan rate of 10 mV/s.

3. Results and discussion

3.1. Surface characteristics of modified carbon materials

Surface functional groups of the prepared Pt/Ru deposited on various carbon supports were studied by XPS measurements. Fig. 1 shows the survey scan spectra for the 0–1100 eV range binding energies for each sample. From the spectra results, the Pt 4f and Ru 3p were prominently found, showing the evidence of Pt/Ru deposition onto carbon samples. In the case of using gas-treated GFs, the intensity of Pt or Ru were enhanced, meaning the increase of Pt or Ru deposition contents. By considering the relative intensity of Pt 4f or Ru 3p, we could conclude that the deposition content was enhanced by increasing the treatment temperature to 200 °C. This increased metal content could be related to the increased in the number of fluorine or oxygen-containing groups

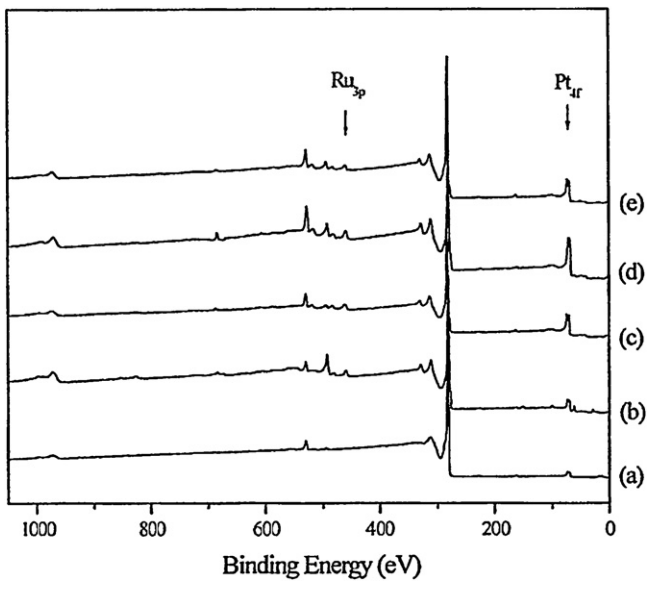

Fig. 1. XPS spectra of PtRu/GFs catalysts using (a) pristine GFs, (b) GFs-RT, (c) GFs-100, (d) GFs-200, and (e) GFs-300.

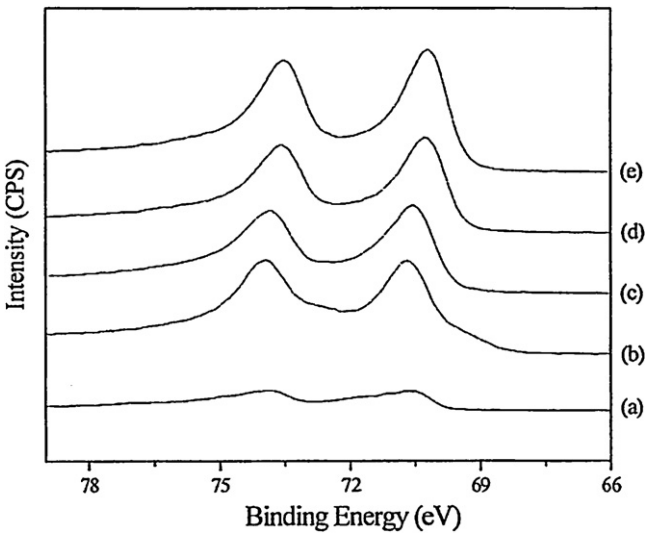

Fig. 2. Pt 4f XPS spectra of PtRu/GFs catalysts using (a) pristine GFs, (b) GFs-RT, (c) GFs-100, (d) GFs-200, and (e) GFs-300.

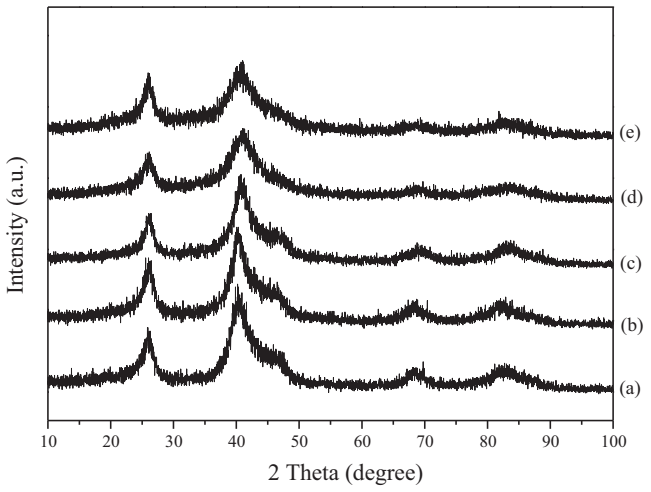

Fig. 3. X-ray diffraction patterns of PtRu/GFs catalysts using (a) pristine GFs, (b) GFs-RT, (c) GFs-100, (d) GFs-200, and (e) GFs-300.

on the GFs surface after treatments. This kind of fluorine or oxygen-containing functional groups addition is similar with previous result [26].

To study the intensity of Pt 4f peak in more detail, the enlarged part spectra for Pt peaks were demonstrated in Fig. 2. This figure also shows the Pt 4f peak intensity for the mixed-gas treated GFs were increased in comparison to that for the pristine GFs. With the increase of treatment temperature from RT to 200 °C, the intensity of Pt was upgraded gradually to a rather small amount. It indicates that the impact of the gas treatment on Pt content is not so highly dependent on the treatment temperature. The more critical factor is whether it is gas treated or not. In the case of gas treatment, the surface functional groups were modified. After gas treatment, GFs gained fluorine or oxygen group and lose some impurities such as hydrogen or sulfur group due to unstable chemical bonds [27]. Gas-treated GFs had similar surface characteristics because Pt 4f peak shape showed little difference with changing temperatures.

Element contents of the gas-treated GFs were investigated by EDS. The results are shown in Table 1. The fluorine and oxygen contents were increased when the treatment temperature of 200 °C, which can be attributed to the increase of fluorine or oxygen containing functional groups of carbon surfaces. During the treatment, fluorine or oxygen diffuses slightly and slowly inside the carbon materials and then the diffusing gas produces active radicals from the carbon backbone during the reaction time because of fluorine or oxygen atom. The active radicals lead to an introduction of fluorine or oxygen functional groups on the carbon materials. The fluorine and oxygen content increased 4.68 and 4.05 wt.%, respectively, when the treatment temperature was 200 °C. In this case of the GFs fluorinated at 300 °C, the fluorine or oxygen content was decreased to 3.97 or 3.42 wt.% in Table 1. This means the higher temperature over 200 °C was not effective for the further modification of surface functional groups. Higher contents of fluorine have been attained on better graphitized structures or higher treatment temperature [27]. This suggests that mixed-gas treatment on carbon materials could bring new fluorine or oxygen content on carbon surface and influence the catalysts deposition.

Table 1
Elemental analysis results of gas-treated GFs as measured by EDS.

	C (wt.%)	F (wt.%)	O (wt.%)
Pristine GFs	97.59	0	1.93
GFs-RT	95.12	1.82	2.76
GFs-100	93.80	2.79	3.31
GFs-200	91.20	4.68	4.05
GFs-300	92.59	3.97	3.42

3.2. Structural characterization of catalysts

The PtRu/GFs catalysts were investigated by XRD to determine the crystal structure of the phase. Fig. 3 shows the XRD patterns of the catalysts deposited carbon materials. The diffraction peak at low angle (20–25°) observed in all XRD patterns are attributed to the diffraction (0 0 2) plane of the carbon support. The other peaks are characteristics of face-centered-cubic (fcc) crystalline Pt, and are indexed with crystalline planes the (1 1 1), (2 0 0), (2 2 0), and (3 1 1), at 2θ values of 40°, 46°, 67°, and 83°, respectively. There are no other distinct reflection peaks in all spectra except those of the four peaks mentioned above, indicating all catalysts had Pt (fcc) crystal structure. XRD patterns of PtRu/carbon materials show only the reflection characteristics corresponding to pure Pt (39.9°) with a little shift of 2θ toward higher values. The angle shifts of the Pt peaks explained an alloy formation between Pt and Ru, which was caused by the incorporation of the base metal in the fcc structure of Pt. No peaks for pure Ru and their oxides were found, but their presence cannot be discarded because they may be present in small amount or even in an amorphous form. An ICP-AES result of carbon materials supported Pt–Ru catalyst has shown an existence of Ru.

The loading contents of Pt and Ru were also measured by the ICP-AES method, and the results are listed in Table 2. The treated GFs at 200 °C showed the highest value, 11.8% (at Pt) and 5.67% (at Ru), whereas the as-received GFs showed the lowest value, 3.42% (at Pt) and 1.23% (at Ru), indicating that in the case of treated GFs, the Pt and Ru loading contents were enhanced. The weight ratio of PtRu was also described in Table 2. The weight ratio was in the range of 1:0.36–1:0.52, meaning the Ru content was increased by the increase of treatment temperature.

The morphologies and particle size distributions of the catalysts were observed by TEM. Fig. 4(a) shows TEM micrographs of the as-received GFs, indicating the fiber morphology having some graphitic structures. Fig. 4(b)–(f) shows the metallic nanoparticles on the surface of GFs, indicating the successful deposition of PtRu particles.

It was found that the catalysts were evenly distributed on the carbon support. The average particle sizes could be obtained by TEM images. In the case of (b) the PtRu/pristine GFs, the image

Table 2
Elemental contents and crystalline sizes of Pt/Ru deposited on GFs.

Supports	Pt (wt.%)[a]	Ru (wt.%)[a]	Pt/Ru ratio	Crystalline size[b] (nm)	Average size[c] (nm)
Pristine GFs	3.42	1.23	1:0.36	3.84	4.9
GFs-RT	6.30	2.52	1:0.40	2.97	4.5
GFs-100	7.84	3.45	1:0.44	2.86	3.2
GFs-200	11.8	5.67	1:0.48	2.31	2.9
GFs-300	10.1	5.24	1:0.52	2.45	2.8

[a] Estimated from ICP-AES method.
[b] Estimated from XRD method.
[c] Estimated from TEM image.

shows 4.1 nm nanoparticles on the surface of the GFs. In contrast to this, in the case of (e) the PtRu/GFs-200 showed the smallest average particle sizes of 2.6 nm with the better dispersion. The uniformity of catalyst particle distribution is known to be important for electrocatalytic activity. Small agglomerates were observed in the dispersion image of carbon supported PtRu nanoparticles, but the presence of individual particles was also observed in enlarged images. This result confirms that the metal particles deposited on the gas-treated carbon material support, is smaller than that of non-treated carbon materials.

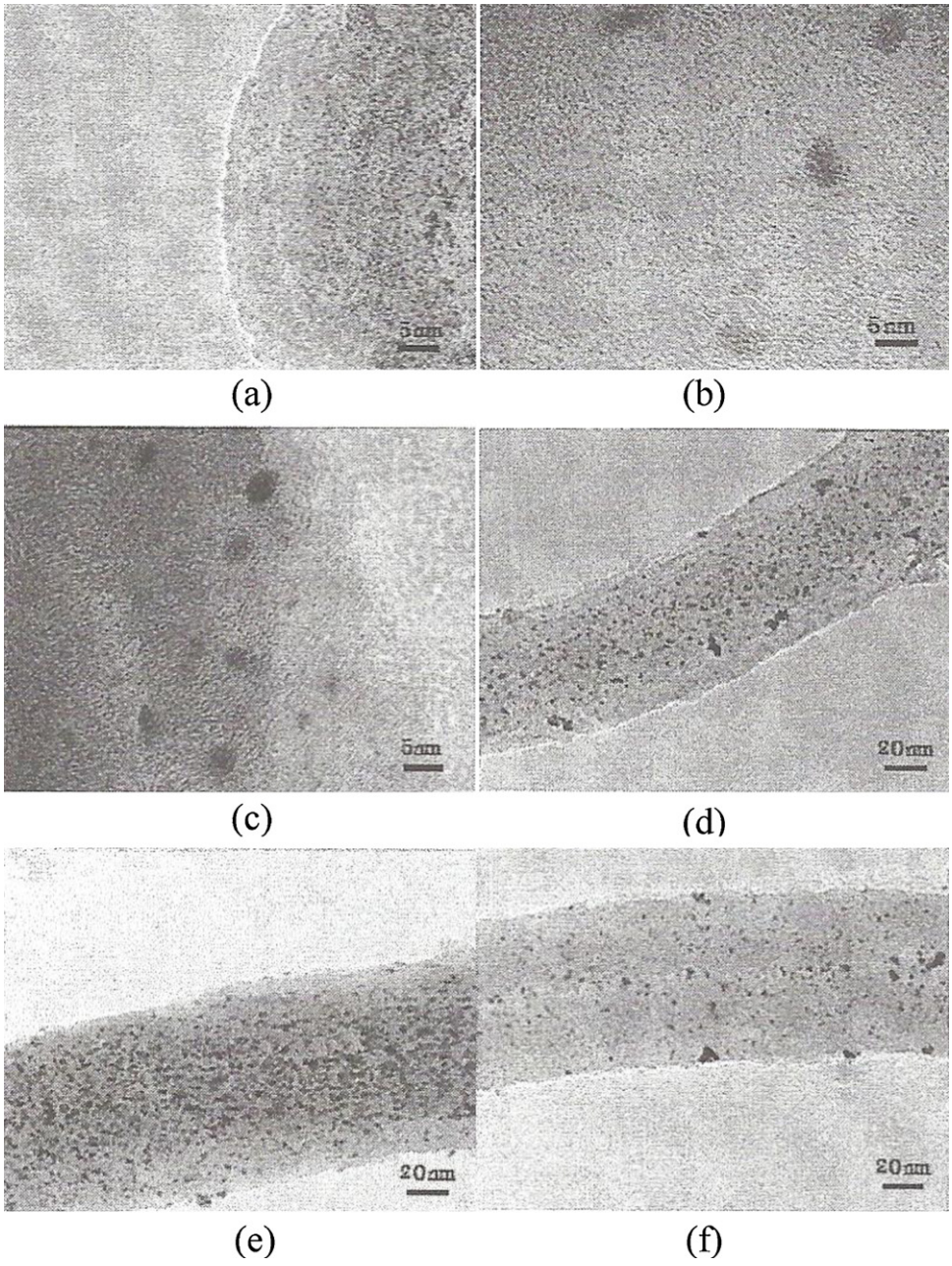

Fig. 4. TEM image of (a) as-received GFs and PtRu/GFs catalysts using (b) pristine GFs, (c) GFs-RT, (d) GFs-100, (e) GFs-200, and (f) GFs-300.

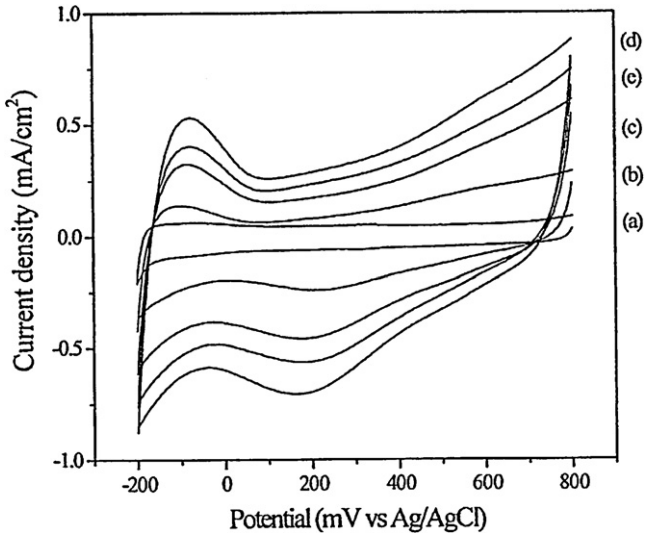

Fig. 5. Cyclic voltammograms of PtRu/GFs catalysts using (a) pristine GFs, (b) GFs-RT, (c) GFs-100, (d) GFs-200, and (e) GFs-300 in 1.0 M H_2SO_4 solution.

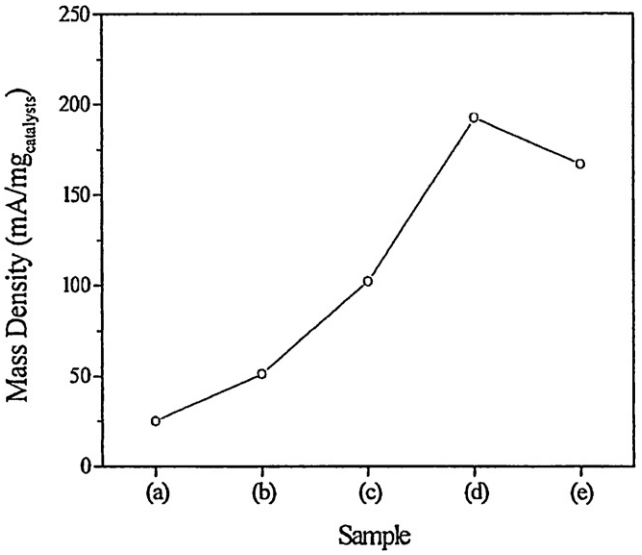

Fig. 7. Current density of PtRu/GFs catalysts using (a) pristine GFs, (b) GFs-RT, (c) GFs-100, (d) GFs200, and (e) GFs-300 in 0.5 M methanol + 1.0 M H_2SO_4 solution.

3.3. Electrochemical characterization

To obtain a specific surface area for an effective redox reaction of catalysts, CVs for the prepared catalysts were performed in 1.0 M sulfuric acid solution and displayed in Fig. 5. After a gas-treatment, the hydrogen adsorption–desorption peaks found in the range of −200 mV to 0 mV increased with increasing treatment temperature to 200 °C. It means that the effective surface area of catalyst was upgraded due to the smaller particle size of catalyst using gas treatment. It could be expected that the catalytic activity will be improved by the enhanced specific surface area of catalyst for a methanol oxidation.

Fig. 6 shows the representative voltammograms of the prepared PtRu/GFs catalysts. It was found that methanol oxidation activity by the PtRu/GFs catalysts was varied with the gas treatment temperature. The voltammetric behaviors were also found to be dependent on the Pt content. In the case of the PtRu/GFs-200, the curve showed a methanol oxidation peak having the largest current density. When the treatment temperature increased to 300 °C, the PtRu/GFs-300 shows the decreased current density toward methanol oxidation. Methanol oxidation was represented by the anodic peak at round 600 mV for catalysts. From this result, it could be concluded that the catalyst on GFs-200 showed the higher current density than any other catalysts. It could be attributed to the difference of surface characteristics, a changed loading content of metal, or metal size of catalysts.

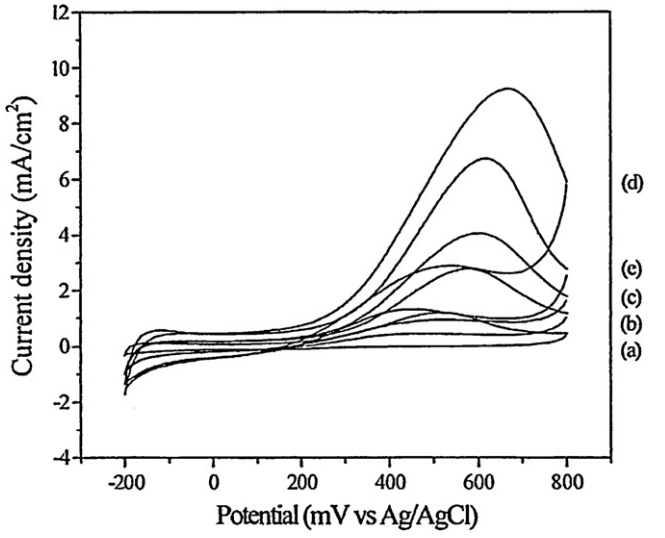

Fig. 6. Cyclic voltammograms of PtRu/GFs catalysts using (a) pristine GFs, (b) GFs-RT, (c) GFs-100, (d) GFs-200, and (e) GFs-300 in 0.5 M methanol + 1.0 M H_2SO_4 solution.

Fig. 7 shows the mass current densities recorded at 600 mV potential of the catalysts, which was obtained from the above CV results. In the case of un-treated GFs, the mass current density was the smallest value of 27 (mA/mg). When the treatment was done at 200 °C, the current density was the highest value of 196 (mA/mg) and in the case of the treatment at 300 °C, the value degraded to 174 (mA/mg). Finally, it could be mentioned that the electro-activity of catalyst was dependent on the particle size and effective surface area.

4. Conclusions

In the present study, the preparation and characterization of PtRu/GFs catalysts were investigated. GFs were modified by gas treatment at several temperatures of RT, 100 °C, 200 °C, 300 °C. GFs treated at 200 °C showed the highest fluorine or oxygen content, meaning an effective modification for the surface characteristics.

In the case of treated GFs supports at 200 °C, the catalyst showed the smallest particle size of 2.31 nm and the highest loading level of Pt (11.8%) and Ru (5.67%). In the case of treated GFs supports at 300 °C, it showed the larger particle size and lower loading level than above sample. It was concluded that particle size and loading content of Pt nanoparticles was dependent on the surface change degree by chemical treatments. It is supported by the EDS result of treated GFs, indicating that the fluorine and oxygen contents were highest value of 4.68 and 4.05 wt.%, respectively, when the treatment temperature was 200 °C.

Accordingly, the PtRu/GFs-200 showed the higher catalytic current densities toward methanol electro-oxidation than any other samples. Consequently, the best electro-catalytic activity was found for the metal catalyst treated at 200 °C. From this result, it could be concluded that small metal particles and high loading of catalysts could lead to an increase in the active areas of catalysts, resulting in good electrocatalytic properties for

methanol oxidation. This result could imply that gas-treated GFs may be a good candidate as a support of the catalyst for methanol oxidation in fuel cells.

Acknowledgments

This research was partly supported by the Converging Research Center Program through the Ministry of Education, Science and Technology (Grant No.: 2012K001261). This research was also partly supported by the Ministry of Knowledge and Economy (Material Source Technology Project, Grant No.: 10037238.2012).

References

[1] K. Bergamaski, E.R. Gonzalez, F.C. Nart, Electrochimica Acta 53 (2008) 4396–4406.
[2] C. Lamy, A. Lima, V.L. Rhun, F. Delime, C. Coutanceau, J.M. Leger, Journal of Power Sources 105 (2002) 283–296.
[3] J. Zhu, Y. Su, F. Cheng, J. Chen, Journal of Power Sources 166 (2007) 331–336.
[4] A.L.M. Reddy, N. Rajalakshmi, S. Ramaprabhu, Carbon 46 (2008) 2–11.
[5] Y.H. Chu, S.W. Ahn, D.Y. Kim, H.J. Kim, Y.G. Shul, H. Han, Catalysis Today 111 (2006) 176–181.
[6] H. Li, G. Sun, L. Cao, L. Jiang, Q. Xin, Electrochimica Acta 52 (2007) 6622–6629.
[7] G. Li, P.G. Pickup, Electrochimica Acta 52 (2006) 1033–1037.
[8] L. Xiong, A. Manthiram, Solid State Ionics 176 (2005) 385–392.
[9] M. Mazurek, N. Benker, C. Roth, H. Fuess, Fuel cells 3 (2006) 208–213.
[10] F. Vigier, C. Coutanceau, F. Hahn, E.M. Belgsir, C. Lamy, Journal of Electroanalytical Chemistry 563 (2004) 81–89.
[11] Y.J. Zhang, A.M. Valiente, I.R. Romos, Q. Xin, A.G. Ruiz, Catalysis Today 93–95 (2004) 619–626.
[12] X. Yu, S. Ye, Journal of Power Sources 172 (2007) 133–144.
[13] T. Kim, S.J. Yang, C.R. Park, Carbon Letters 12 (2011) 194–206.
[14] S. Kim, S.J. Park, Solid State Ionics 178 (2008) 1915–1921.
[15] B.J. Kim, Y.S. Lee, S.J. Park, Current Applied Physics 8 (2008) 736–738.
[16] G. Wu, Y.S. Chen, B.Q. Xu, Electrochemistry Communications 7 (2005) 1237–1243.
[17] J.H. Choi, K.W. Park, H.K. Lee, Y.M. Kim, J.S. Lee, Y.E. Sung, Electrochimica Acta 48 (2003) 2781–2789.
[18] W. Li, C. Liang, W. Zhou, J. Qiu, Z. Zhou, G. Sun, Q. Xin, Journal of Physical Chemistry B 107 (2003) 6292–6299.
[19] D. Shin, S. Bae, C. Yan, J. Kang, J. Ryu, J.H. Ahn, B.H. Hong, Carbon Letters 13 (2012) 1–16.
[20] G. Girishkumar, T.D. Hall, K. Vinodgopal, P.V. Kamat, Journal of Physical Chemistry B 110 (2006) 107–114.
[21] Y.J. Jung, S. Kim, S.J. Park, J.M. Kim, Colloids and Surfaces A: Physicochemical and Engineering Aspects 313–314 (2008) 167–170.
[22] S.J. Park, Y.S. Jang, Journal of Colloid and Interface Science 237 (2001) 91–97.
[23] Y.S. Lee, B.K. Lee, Carbon 40 (2002) 2461–2468.
[24] A. Bismarck, R. Tahhan, J. Springer, A. Schulz, T.M. Klapotke, H. Zell, W. Michaeli, Journal of Fluorine Chemistry 84 (1997) 127–134.
[25] Z. Liu, X.Y. Ling, B. Guo, L. Hong, J.Y. Lee, Journal of Power Sources 167 (2007) 272–280.
[26] M.J. Jung, E. Jeong, S. Kim, S.I. Lee, J.S. Yoo, Y.S. Lee, Journal of Fluorine Chemistry 132 (2011) 1127–1133.
[27] J.S. Im, S.J. Park, Y.S. Lee, International Journal of Hydrogen Energy 34 (2009) 1423–1428.